Annals of Biomedical Engineering, Vol. 29, pp. 427–435, 2001
Printed in the USA. All rights reserved.

0090-6964/2001/29(5)/427/9/$15.00

Dielectrical Model of Cellular Structures in Radio Frequency and Microwave Spectrum. Electrically Interacting Versus Noninteracting Cells

SERGUEI Y. SEMENOV,[1] GALINA I. SIMONOVA,[2] ANDREY N. STAROSTIN,[2] MICHAEL G. TARAN,[2] ALEXANDER E. SOUVOROV,[1] ALEXANDER E. BULYSHEV,[1] ROBERT H. SVENSON,[1] ALEXEI G. NAZAROV,[3] YURI E. SIZOV,[2] VITALY G. POSUKH,[4] ANDREY PAVLOVSKY,[3] and GEORGE P. TATSIS[1]

[1]Laser and Applied Technologies Laboratory, Carolinas Heart Institute and Carolinas Medical Center, 1000 Blythe Boulevard, Charlotte, NC, [2]Troitsk Institute of Thermonuclear and Innovative Research, Troitsk, Moscow Region, Russia, [3]Kurchatov Institute of Atomic Energy, 2 Kurchatov sq., Moscow, Russia, and [4]Institute of Laser Physics, Novosibirsk, Russia

(Received 21 June 2000; accepted 15 February 2001)

Abstract—A model of dielectrical properties of cellular structures of a tissue has been proposed. Cellular structures were presented as a composition of membrane covered spheres and cylinders that do not interact with each other. No restrictions were applied to the thickness of cellular membranes. The model was further generalized into a case of electrically interacting cells. The difference in dielectrical properties calculated with the model of electrically noninteracting versus interacting cells is inversely dependent on frequency. At biological values of cellular volume fraction near 0.7 (packed configuration) the difference is about 10%–15% in resistance and in ϵ' for frequencies near 0.1 MHz. Experimental data for myocardial tissue and theoretical data, for both interacting and noninteracting models, reasonably agree at frequencies of 1–100 MHz. © *2001 Biomedical Engineering Society.*
[DOI: 10.1114/1.1366675]

Keywords—Dielectrical properties and relaxation, Cellular structures, Composite model.

INTRODUCTION

The dielectrical properties of biological tissues in the radio frequency and microwave spectrum have been studied.[6–8,22,27] The need for these properties to be known comes from the development of a variety of new biomedical technologies, including tomography and hyperthermia.[17,20,21,23,24] It has been shown, that *in situ* tissue dielectrical properties are strongly affected by their physiological and pathological conditions.[4,14,25,29] We have experimentally demonstrated such dependencies during acute ischemia and chronic infarction on canine models in the microwave spectrum from 0.2 to 6.0 GHz.[25] The functional dependencies of myocardial impedance properties have also been studied in the low frequency region.[4]

The theoretical basis for interpretation of experimentally measured changes in the myocardial dielectrical/impedance properties during various physiological and pathological interventions still remains unclear. This interpretation requires a realistic model of dielectrical properties of myocardial tissue as a cellular composition. Different dielectrical models of cellular tissue structure have been suggested.[2,6,9,10,12] The major simplification used in these developed models is that cells were assumed to be electrically noninteracting with each other. It is clear that such an assumption would provide better agreement with the experimental data for a low cellular volume fraction. However, the degree of uncertainty of such a simplification in modeling of tissues with packing cellular composition is not understood.

The first objective of this study was development of models of dielectrical properties of myocardial tissue as a composition of both electrically interacting and noninteracting cells. The second objective was to compare these and previously developed models, composed of various cellular volume fractions with each other and with experimental data. The major focus of this research was in the development of mathematical models and computer simulations. Experimental data were taken from *in situ* acute studies on canines (Experimental Methods section). The models for electrically noninteracting and interacting cells are presented in model 1 and model 2 section, respectively. Comparisons of the different models with each other and with experimental data are presented in the Results and Discussion section.

Address correspondence to: Serguei Y. Semenov, PhD, Laser and Applied Technologies Laboratory, Carolinas Medical Center, 1000 Blythe Boulevard, Charlotte, NC 28203-2861. Electronic mail: ssemenov@carolinas.org

EXPERIMENTAL METHODS

The experimental data have been obtained in experiments with 13 canines, of either sex with average weight of about 30 kg. The experimental procedure has been presented in detail elsewhere.[25] Animals were part of an Institutional Animal Care and Use Committee approved research protocol and cared for under NIH guidelines for laboratory research.[11] All animals were premedicated with 1 mg acepromazine, and 0.3 mg/kg butorphanol IM, 20 min prior to an aesthetic induction. The animals were anesthetized with 15 mg/kg thiopental intravenously. Following induction, the animals were intubated and placed on a volume control respirator. Anesthesia was maintained with 0.5%–3% isoflurane. An expired CO_2 monitor, lead II EKG, and arterial blood pressure were utilized to monitor the animal. An intravenous line was placed in the peripheral vein for administration of fluids and drugs. The right groin and left chest were surgically prepped and draped. A thoracotomy was made in the fifth intercostal space. The pericardium was open to expose the epicardial surface of the left ventricular myocardium.

Dielectrical properties were measured with the help of a coaxial microwave probe manually placed on the epicardium during a single multifrequency interrogation. The probe was an open end of coaxial line with inner diameter of 0.6 mm and outer diameter of 3.0 mm. It was estimated that the probe interrogation of the myocardium approximated a cylinder 10 mm in diameter and 2.5–3.0 mm in depth. Precautions were taken to avoid blood or saline introduction between the microwave probe and the myocardium. The microwave probe was connected to a Hewlett-Packard Network Analyzer (HP Model No. 8753C). We used our own developed software and calibration procedures to measure myocardial dielectrical properties in the frequency range 0.1 MHz–6.0 GHz. We have conducted 231 measurements at each frequency point. All values were expressed as mean ± one standard deviation (SD).

MODELING OF BULK DIELECTRICAL PERMITTIVITY OF MYOCARDIAL TISSUE AS A COMPOSITION OF NONINTERACTING MEMBRANE COVERED CELLS (MODEL 1)

The dielectrical models of biological tissue as a composition of membrane covered spheres are based on the Maxwell[19] theory, which was further generalized by Foster and Schwan.[6] In addition to the assumption that cells do not electrically interact with each other, they used a simplification on small parameter h/R (where h is a membrane thickness and R is radius of a cell). Using this approach as a classic model, we developed a model without any restriction on the ratio of h/R. In addition to this, such a model allows further generalization into the case of electrically interacting cells. The generalization has been completed (model 2 section).

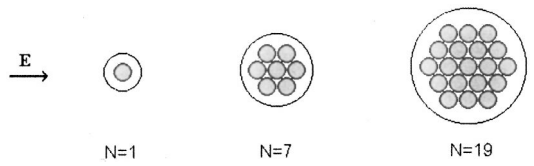

FIGURE 1. Geometrical configuration of non-interacting cells problem ($N=1$) and the interacting cells problem for packed configuration of 7 cells ($N=7$) and 19 cells ($N=19$).

Let us consider a homogeneous and isotropic medium in which identical cells occupy pth part of the volume (Fig. 1, $N=1$). We consider spherical or an infinite cylindrical shape of cells with radius r_1. Each cell has a membrane with thickness (h). Further, we use indexes 0, 1, and 2 for marking intracellular, membrane, and extracellular properties, respectively. Dielectrical properties of intracellular (ϵ_0), membrane (ϵ_1), and extracelluar (ϵ_2) spaces were considered to be homogeneous and identical for all cells. For such a media, we considered the case for irradiating by plane electromagnetic wave [with time dependence $e^{-i\omega t}$ ($\omega=2\pi f$)], with frequency f (Hz), and amplitude E^0 (V/m). The problem is to define bulk (effective) dielectrical permittivity ϵ_{eff} and conductivity σ_{eff} of such a mixture.

An effective (bulk) dielectrical permittivity of mixture ϵ_{eff} was defined[16] as a coefficient between mean (by volume) values of D and E: $\overline{D}=\epsilon_{\text{eff}}E$. Here overbar defines volume averaging. For isotropic media we can obtain

$$\begin{aligned}\epsilon_{\text{eff}} &= \int_V D(r)dr \Big/ \int_V E(r)dr \\ &= \left[\epsilon_0\int_{V_0}E(r)dr+\epsilon_1\int_{V_1}E(r)dr+\epsilon_2\int_{V_2}e(r)dr\right]\Big/ \\ &\quad \left[\int_{V_0}E(r)dr+\int_{V_1}E(r)dr+\int_{V_2}E(r)dr\right] \\ &= \epsilon_2+\left[(\epsilon_0-\epsilon_2)\int_{V_0}E(r)dr+(\epsilon_1-\epsilon_2)\right. \\ &\quad \left.\times\int_{V_1}E(r)dr\right]\Big/\left[\int_{V_0}E(r)dr\right. \\ &\quad \left.+\int_{V_1}E(r)dr+\int_{V_2}E(r)dr\right], \qquad (1)\end{aligned}$$

where volume integrals are taken inside of the intracellular sphere (V_0), the membrane shell (V_1), and the extracelluar shell with volume $V_2=(V_0+V_1)(1-p)/p$ in the three-dimensional case. In the two-dimensional case of cylindrical geometry the integrals were taken inside of corresponding circle and rings.

Let us assume that (1) the interactions between cellular structures and (2) the changes of electrical field within extracelluar space $[E^{(2)}]$ can be neglected. (Approximation of electrically noninteracting cells.) In this case the mean internal fields within cells are identical and equal to $E^{(s)}$, $s=0,1$. As will be shown later, directions of all mean fields are identical to the incident field. In this case $\int_{V_s} E(r)dr=V_s E^{(s)}$, where $\overline{E}^{(s)}$—mean electrical field in the sth layer.

Applying this approximation to Eq. (1), it is easy to obtain

$$\epsilon_{\text{eff}}=\epsilon_2+p\,\frac{(\epsilon_0-\epsilon_2)\dfrac{r_0^d}{r_1^d}\overline{E}^{(0)}+(\epsilon_1-\epsilon_2)\left(1-\dfrac{r_0^d}{r_1^d}\right)\overline{E}^{(1)}}{p\dfrac{r_0^d}{r_1^d}\overline{E}^{(0)}+p\left(1-\dfrac{r_0^d}{r_1^d}\right)\overline{E}^{(1)}+(1-p)\overline{E}^{(2)}}, \tag{2}$$

where d—dimension of space [(2)—for cylindrical cells and (3)—for spherical cells], $r_0=r_1-h$ is the inner radius of cell.

Within the radio frequency and microwave spectrum, the wavelength of electromagnetic fields is much greater than cellular diameter. In this case, the problem can be solved in the electrostatic approximation using Laplace equation in R^d for field potential in a three-component medium. (We compared results of electrostatic and vector wave fields approaches for spherical cells and found that within a spectrum of $f<30\,\text{GHz}$ mean electrical fields agree with four orders.) Let the incident field be E^0. Having $E=-\text{grad}[u(r,\theta)]$, let us solve the problem for field potential $u(r,\theta)$.

The field potential can be found as[16]

$$u(r,\theta)=\begin{cases} u_0(r,\theta)=-A_0E^0r\cos(\theta), & r\leqslant r_0, \\ u_1(r,\theta)=-A_1E^0\left(r-\dfrac{B_1}{r^{d-1}}\right)\cos(\theta), & \\ \qquad\qquad r_0<r\leqslant r_1, & \\ u_2(r,\theta)=-E^0\left(r-\dfrac{B_2}{r^{d-1}}\right)\cos(\theta), & r>r_1 \end{cases}, \tag{3}$$

where θ—angle between the direction of the electromagnetic field and the radius vector. Unknown coefficients can be found from boundary conditions (continuity of u and $\epsilon\partial u/\partial r$):

$$b_1=\frac{(\epsilon_0-\epsilon_1)}{\epsilon_0+(d-1)\epsilon_1}r_0^d,$$

$$B_2=\frac{(\epsilon_1-\epsilon_2)[\epsilon_1+(d-1)\epsilon_1]r_1^d+(\epsilon_0-\epsilon_1)[\epsilon_1+(d-1)\epsilon_1]r_0^d}{[\epsilon_0+(d-1)\epsilon_1][\epsilon_1+(d-1)\epsilon_2]r_1^d+(d-1)(\epsilon_0-\epsilon_1)(\epsilon_1-\epsilon_2]r_0^d}r_1^d, \tag{4}$$

$$A_1=\frac{d\epsilon_2[\epsilon_0+(d-1)\epsilon_1]r_1^d}{[\epsilon_0+(d-1)\epsilon_1][\epsilon_1+(d-1)\epsilon_2]r_1^d+(d-1)(\epsilon_0-\epsilon_1)(\epsilon_1-\epsilon_2]r_0^d},$$

$$A_0=\frac{d\epsilon_1}{\epsilon_0+(d-1)\epsilon_1}A_1.$$

It is easy to show that mean fields in each layer are directed along the incident field (x axis) and equal to

$$\overline{E}_x^{(0)}=A_0E^0,\quad \overline{E}_x^{(1)}=A_1E^0,\quad \overline{E}_x^{(2)}=E^0. \tag{5}$$

Substituting Eqs. (3)–(5) in Eq. (2) we find

$$\epsilon_{\text{eff}}=\epsilon_2+p\epsilon_2 d\frac{(\epsilon_1\epsilon_2)[\epsilon_0+(d-1)\epsilon_1]+(\epsilon_0-\epsilon_1)[\epsilon_2+(d-1)\epsilon_1]\frac{r_0^d}{r_1^d}}{[\epsilon_0+(d-1)\epsilon_1]\{[\epsilon_1+(d-1)\epsilon_2]+p(\epsilon_2-\epsilon_1)\}+\frac{r_0^d}{r_1^d}(\epsilon_0-e_1)\{(d-1)(\epsilon_1-\epsilon_2)-p[(d-1)\epsilon_1+\epsilon_2]\}}. \tag{6}$$

MODELING OF BULK DIELECTRICAL PERMITTIVITY OF MYOCARDIAL TISSUE AS A COMPOSITION OF MEMBRANE COVERED INTERACTING CELLS (MODEL 2)

Let us suppose that N cells exist in a cylindrical volume V_R (cylinder with radius R). The geometrical configuration of cellular structures in its packed position is presented in Fig. 1 for 7 cells ($N=7$) and for 19 cells ($N=19$). In this part we model a myocardial cell as an infinite, membrane covered cylinder with radius $\tilde{a}_s=a_s+h_s$, where h_s is a thickness of the membrane of the cell number s. Axes of the cylinders are parallel to each other and coaxial to OZ, $E=(E^0,0,0)$. Here we are making an assumption that cells do electrically interact with each other. The problem is to define the bulk (effective) dielectrical permittivity ϵ_{eff} and conductivity σ_{eff} of such a mixture.

Similar to before, we will solve the problem in an electrostatic approximation using Laplace equation in R^2 for field potential in a three-layered medium. To find a solution for this problem, we will use the approach proposed in Ref. 13. The field potential for intracellular [Eq. (7)], membrane [Eq. (8)], and extracellular [Eq. (9)] spaces can be found as

$$U_0^s(r,\varphi)=-\left[A_0^s+\sum_{n=1}^{\infty}(A_n^s z_s^n+\tilde{A}_n^s\overline{z_s}^n)\right],\quad r_s=|z_s|<a_s; \tag{7}$$

$$U_1^s(r,\varphi)=-\left\{B_0^s+\sum_{n=1}^{\infty}[(B_n^s z_s^n+C_n^s\overline{z_s}^n)+(\tilde{B}_n^s\overline{z}_s^n+\tilde{C}_n^s z_s^{-n})]\right\},\quad a_s<r_s<\tilde{a}_s; \tag{8}$$

$$U_2(r,\varphi)=-\left[\left(\frac{E^0}{2}z+\frac{E^0}{2}\overline{z}\right)+\sum_{s=1}^{N}\sum_{n=1}^{\infty}(F_n^s\overline{z_s}^n+\tilde{F}_n^s z_s^{-n})\right],$$

$$z\in V_R\setminus\bigcup_{s=1}^{N}\tilde{V}_s,\quad \tilde{V}_s=V_s\cup m_s. \tag{9}$$

(V_s and m_s are volumes of sth cell and its membrane, respectively) with unknown coefficients

$$A_n^s,\quad B_n^s,\quad C_n^s,\quad F_n^s,\quad \tilde{A}_n^s,\quad \tilde{B}_n^s,\quad \tilde{C}_n^s,\quad \tilde{F}_n^s,\quad s=1,...,N, \tag{10}$$

where $z=re^{i\varphi}$, $\overline{z}=re^{-i\varphi}$, $z_s=r_s e^{i\varphi_s}=z-z_{0s}$, z_{0s}—is the center of sth cell, $n=0,\pm1,\pm2,...,m_s$ is the volume of the sth membrane.

Here we have $8N$ unknown coefficients [Eq. (10)] for each decomposition coefficient n. Also, we have two types of boundary conditions for continuity U and $\epsilon(\partial U/\partial r)$ that have to be satisfied on each of $2N$ boundaries for the whole range of angles $\varphi\in[0,2\pi]$. Therefore, $8N$ unknown coefficients can be found from $8N$ boundary equations. After substitutions of variables

$$\begin{cases}\hat{F}_n^s=F_n^s/(\tilde{a}_s)^n,\\ \bar{\hat{F}}_n^s=\tilde{F}_n^s/(\tilde{a}_s)^n,\end{cases} \tag{11}$$

and some transformations, we obtain an infinite linear equation system in variables $\hat{F}_n^s$, $\bar{\hat{F}}_n^s$, $s=1,...N$:

$$\begin{cases}\tilde{\kappa}_n^s\hat{F}_n^s=\sum_{j\neq s}(-1)^n\sum_{m=1}^{\infty}\binom{m+n-1}{n}\times\bar{\hat{F}}_m^j\frac{\tilde{a}_j^m\tilde{a}_s^n}{z_{js}^{m+n}}+\frac{E^0}{2}\tilde{a}_s\chi(n=1),\\ \tilde{\kappa}_n^s\bar{\hat{F}}_n^s=\sum_{j\neq s}(-1)^n\sum_{m=1}^{\infty}\binom{m+n-1}{n}\times\hat{F}_m^j\frac{\tilde{a}_j^m\tilde{a}_s^n}{\overline{z_{js}}^{m+n}}+\frac{E^0}{2}\tilde{a}_s\chi(n=1),\\ s=1,...,N\end{cases} \tag{12}$$

where $\binom{m+n-1}{n}=C_{m+n-1}^n=[(m+n-1)!]/[n!(m-1)!]$—binomial coefficients,

$$\chi(n=1)=\begin{cases}1, & n=1\\ 0, & n\neq1\end{cases},\quad z_{js}=z_j-z_s,$$

and

$$\left|\frac{\tilde{a}_j}{z_{js}}\right|<1, \quad \left|\frac{\tilde{a}_s}{z_{js}}\right|<1,$$

$$\tilde{\kappa}_n^s=\frac{\alpha_n^s+(\epsilon_1^s/\epsilon_2)\beta_n^s}{\alpha_n^s-(\epsilon_1^s/\epsilon_2)\beta_n^s}, \tag{13}$$

$$\begin{cases} \alpha_n^s=\frac{1}{2}\left(1+\frac{\epsilon_0^s}{\epsilon_1^s}\right)+\frac{1}{2}\left(1-\frac{\epsilon_0^s}{\epsilon_1^s}\right)\left(\frac{a_s}{\tilde{a}_s}\right)^{2n}, \\ \beta_n^s=\frac{1}{2}\left(1+\frac{\epsilon_0^s}{\epsilon_1^s}\right)-\frac{1}{2}\left(1-\frac{\epsilon_0^s}{\epsilon_1^s}\right)\left(\frac{a_s}{\tilde{a}_s}\right)^{2n}. \end{cases} \tag{14}$$

Solving this system of equations by cutting method and increasing the system dimensions until a solution is stabilized, the unknown coefficients F_n^s, $\tilde{F}_n^s$ can be found. Another $6N$ unknown coefficients [Eq. (10)] are expressed from F_n^s, $\tilde{F}_n^s$:

$$\begin{cases} A_n^s=\frac{2(\tilde{a}_s)^{-2n}}{\alpha_n^s-(\epsilon_1^s/\epsilon_2)\beta_n^s}F_n^s, \\ \tilde{A}_n^s=\frac{2(\tilde{a}_s)^{-2n}}{\alpha_n^s-(\epsilon_1^s/\epsilon_2)\beta_n^s}\tilde{F}_n^s, \end{cases} \tag{15}$$

$$\begin{cases} B_n^s=\frac{1}{2}\left(1+\frac{\epsilon_0^s}{\epsilon_1^s}\right)A_n^s, \quad \tilde{B}_n^s=\frac{1}{2}\left(1+\frac{\epsilon_0^s}{\epsilon_1^s}\right)\tilde{A}_n^s, \\ C_n^s=(a_s)^{2n}\frac{1}{2}\left(1-\frac{\epsilon_0^s}{\epsilon_1^s}\right)A_n^s, \quad \tilde{C}_n^s=(a_s)^{2n}\frac{1}{2} \\ \qquad\qquad \times\left(1-\frac{\epsilon_0^s}{\epsilon_1^s}\right)\tilde{A}_n^s. \end{cases} \tag{16}$$

The average intracellular [Eq. (17)] membrane [Eq. (18)], and extracellular [Eq. (19)] fields are found, respectively,

$$\begin{cases} \int_{|z_s|<a_s} E_x^{(0,s)}dV=\frac{2(\tilde{a}_s)^{-2n}}{\alpha_1^s-(\epsilon_1^s/\epsilon_2)\beta_1^s}(F_1^s+\tilde{F}_1^s)\pi a_s^2, \\ \int_{|z_s|<a_s} E_y^{(0,s)}dV=\frac{2(\tilde{a}_s)^{-2n}}{\alpha_1^s-(\epsilon_1^s/\epsilon_2)\beta_1^s}i(F_1^s-\tilde{F}_1^s)\pi\alpha_s^2, \end{cases} \tag{17}$$

$$\begin{cases} \int_{a_s<|z_s|<\tilde{a}_s} E_x^{(1,s)}dV=(1+\epsilon_0^s/\epsilon_1^s)\frac{(\tilde{a}_s)^{-2n}}{\alpha_1^s-(\epsilon_1^s/\epsilon_2)\beta_1^s} \\ \qquad\qquad \times(F_1^s+\tilde{F}_1^s)\pi(\tilde{\alpha}_s^2-a_s^2), \\ \int_{a_s<|z_s|<\tilde{a}_s} E_y^{(1,s)}dV=(1+\epsilon_0^s/\epsilon_1^s)\frac{(\tilde{a}_s)^{-2n}}{\alpha_1^s-(\epsilon_1^s/\epsilon_2)\beta_1^s} \\ \qquad\qquad \times i(F_1^s-\tilde{F}_1^s)\pi(\tilde{\alpha}_s^2-a_s^2), \end{cases} \tag{18}$$

$$\int_{V_R\setminus(\bigcup_{s=1}^{N}\tilde{V}_s)} E_x^{(2)}dV=E^0\pi R^2-\sum_{s=1}^{N}\kappa_1^s(F_1^s+\tilde{F}_1^s)\pi\tilde{a}_s^2, \tag{19}$$

$$\int_{V_R\setminus(\bigcup_{s=1}^{N}\tilde{V}_s)} E_y^{(2)}dV=-i\sum_{s=1}^{N}\kappa_1^s(F_1^s-\tilde{F}_1^s)\pi\tilde{a}_s^2,$$

where $\kappa_1^s=\tilde{\kappa}_1^s(\tilde{a}_s)^{-2}$, $\tilde{\kappa}_1^s$ from Eq. (13), $i^2=-1$.

Summarizing Eqs. (17), (18), and (19), we obtain a mean by volume complex dielectrical permittivity $\overline{\epsilon_x}=(\int_{V_R}\epsilon E_x dV/\int_{V_R}E_x dV)$:

$$\int_{V_R}E_x dV=\pi\sum_{s=1}^{N}\frac{(F_1^s+\tilde{F}_1^s)}{\alpha_1^s-(\epsilon_1^s/\epsilon_2)\beta_1^s} \times\left\{2\frac{a_s^2}{\tilde{a}_s^2}+(1+\epsilon_0^s/\epsilon_1^s)\left(1-\frac{a_s^2}{\tilde{a}_s^2}\right) -[\alpha_1^s+(\epsilon_1^s/\epsilon_2)\beta_1^s]\right\}+\pi E^0R^2, \tag{20}$$

$$\int_{V_R}\epsilon E_x dV=\pi\sum_{s=1}^{N}\frac{(F_1^s+\tilde{F}_1^s)}{\alpha_1^s-(\epsilon_1^s/\epsilon_2)\beta_1^s}\left\{2\frac{a_s^2}{\tilde{a}_s^2}\epsilon_0^s+(1+\epsilon_0^s/\epsilon_1^s) \times\left(1-\frac{a_s^2}{\tilde{a}_s^2}\right)\epsilon_1^s-[\alpha_1^s+(\epsilon_1^s/\epsilon_2)\beta_1^s]\epsilon_2\right\} +\pi E^0R^2\epsilon_2.$$

The accuracy of the solution depends on the number of decomposition n. We compared solution for $n=10$, 20, 30, 50, and 60 at frequency spectrum from 10 kHz up to 8 GHz for normal cellular properties with volume fraction of 0.68. Results for $n=50$ and $n=60$ are equivalent with an accuracy of 0.1%. Most of the differences between low and high values of n were found at low frequencies. For example, the relative error between $n=10$ and $n=50$ at 10 kHz were 2% for ϵ' and 0.8% for resistance ρ. In the case of $n=20$, these errors were 0.6% and 0.2%, respectively. Therefore, it was concluded that to obtain results with relative error of about

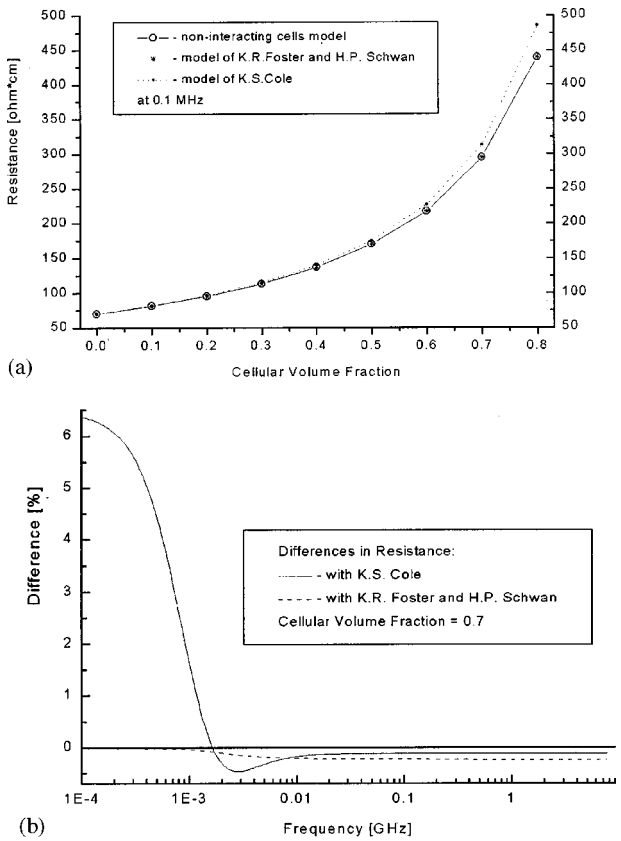

FIGURE 2. (a) The dependencies of bulk resistance at 0.1 MHz from cellular volume fraction, obtained with different models. (b) Frequency dependent percent differences in bulk resistance obtained with different models at a cellular volume fraction 0.7.

1% it is sufficient to have $n=20$. This number can be significantly lower for higher frequencies.

RESULTS AND DISCUSSION

In order to calculate bulk myocardial properties, the dielectrical properties of intracellular, membrane, and extracellular volumes have to be known. Choice of these properties and other parameters of the model are given in the Appendix and will be further referenced as a set of standard parameters of a model.

First, we compared our noninteracting cell model (model 1) with previously published models. Results for bulk resistance comparing our noninteracting cell model with two classical models are presented in Fig. 2(a) for a frequency of 0.1 MHz as a function of cellular volume fraction. The results were also compared at frequency spectrum for a biological value of cellular volume fraction of 0.7 [Fig. 2(b)]. At a whole range of frequencies our results agree well with the proposed model of Foster and Schwan [Eqs. (44) and (53) from Ref. 6]. This can be seen in both Figs. 2(a) and 2(b). This underlines that at ratio h/R near 10^{-3}, a simplification of the first order of this parameter can be used. It is appropriate for myocardial tissue that has the ratio of h/R about 10^{-3}–10^{-4}. At higher membrane thickness or at lower cellular dimensions, for example in the case of small ribosome-like structures with the ratio of h/R about 10^{-1} or higher, the difference between these two models became more significant. This leads to necessity of not using a simplified model. In a limit of $h/R \to 0$ our model is equivalent to the previously developed approach [Eq. (44) in Ref. 6].

As was expected, at frequencies significantly higher than the relaxation frequency of cellular membranes (near 1–10 MHz), when the cellular membrane becomes transparent to the electromagnetic field, results also agree with the model proposed by Cole.[2] This can be seen in Fig. 2(b). At lower frequencies, when the cellular membrane plays an important role, and at higher cellular concentrations the difference with the model of Cole slightly increases. Therefore, it was concluded that our model gives reasonable results, comparable with previously developed approaches. Further, we generalized our model to take into account an electrical interaction between cells (Model 2 section).

An approach for calculation of concentrated suspension of membrane covered spheres was proposed.[12] The approach is based on two steps modeling. First, shelled sphere is replaced by homogeneous sphere with an effective dielectrical permittivity calculated based on the Maxwell theory.[19] Second, the bulk dielectrical permittivity of concentrated spheres is calculated. However, such an approach has limited usage, because of the initial approximation used in the first step. It is an approximation of uniform field in which the sphere is located, that allows to find a solution for an induced dipole. In the case of concentrated suspension, it is no longer the true—the field is nonuniform. In a nonuniform field all multipoles have to be counted, which was done here in model 2.

The dielectrical properties of models 1 and 2 are compared in Fig. 3(a) for bulk ϵ' and in Fig. 3(b) for bulk resistance (ρ). The parameters of the models were standard. Model 2 is presented for two cases: 7 and 19 cells in a cluster. The difference between interacting and noninteracting cellular models is frequency dependent. The more pronounced differences are in low frequency region, because of the membrane influence. However, the difference is not large; up to 10%–15% in resistance and in ϵ', even for the case when cellular volume fraction is in a range of biological values near 0.7, for example, for myocardial tissue.

As can be seen from Fig. 3, in packed cellular configuration (high cellular volume fraction), the solution is stabilized in about a dozen cells in a cluster. In less packed configuration the situation is quite different. It may depend on a structure itself. For example, in the

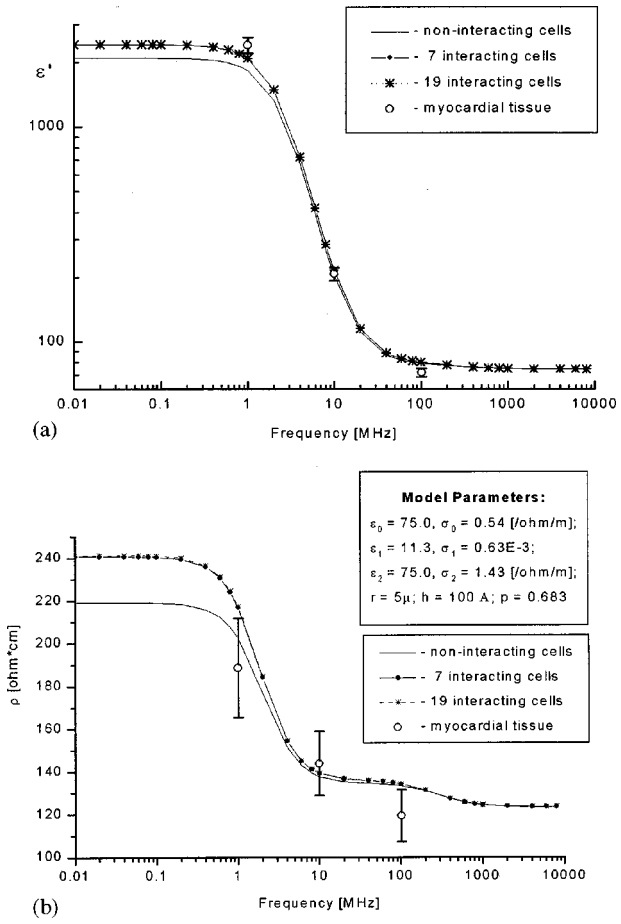

FIGURE 3. Comparison of the experimental data for myocardial tissue (N_{exp}=231) with noninteracting cells model and with interacting cells model at different numbers of cells in a cluster for: ϵ'—in (a) and ρ—in (b).

case of two cells when the line between centers of cells has a different angle with the electrical vector, the difference in bulk dielectrical properties can be significant at low frequencies for both ϵ' and ρ. In other words, in nonpacked cellular configurations, dielectrical properties are different in cases when the same number of cells are positioned differently (structural anisotropy). At higher frequencies (>10 MHz), the dielectrical properties of cellular structures are less anisotropic. It has to be emphasized, that we define an effective (bulk) dielectrical permittivity of mixture ϵ_{eff} similar to Ref. 16 as a coefficient between mean (by volume) values of D and E: $\overline{D} = \epsilon_{\text{eff}} \overline{E}$ [Eq. (1)]. In this particular case of two interacting cells this means that we consider an infinite amount of double-interacting cells.

Results of modeling were compared with experimentally measured data. Results are presented for ϵ' and ρ in Figs. 3(a) and 3(b), respectively. Presented models do not take into account the high frequency components of protein, bound water and free relaxations, that were previously considered.[26] They also do not include low frequency relaxation of subcellular components. Therefore, it is understood that experimental and theoretical data can be compared at frequencies near the cellular membrane relaxation spectrum. This comparison is presented in Fig. 3 for frequencies from 1 to 100 MHz. Experimental data are presented as a mean ± one SD for a group of 13 canines, combining 231 measurements at each frequency point. The experimental data were obtained in a large number of *in situ* experiments with significant individual variation in local blood supply, reaction on anesthesia, probe position in relation to blood vessels, intramural inhomogeneity, etc. This explains relatively high deviations (up to 12%) in experimental data, presented in Fig. 3. Experimental and theoretical data, for both interacting and noninteracting models, reasonably agree. However, no conclusion can be made that agreement is better for interacting cells rather than for noninteracting cells. Differences between models are in the same order as a difference between experimental and theoretical data. To analyze dielectrical spectroscopy data at a wide radio frequency and microwave spectrum, the model of interacting cells needs to be further developed to incorporate both higher frequency and lower frequency relaxation components and also a distribution of relaxation times.

We used a model of infinite cylinders with a circular cross section for simulation of myocardial cellular composition. This model allows us to estimate an effect of electrical interaction of cells on bulk dielectrical properties of tissue. Cardiac cells do not have an ideal circular cross section. The model of electrical conductivity of skeletal muscle utilizing a hexagonal cross section of the cells was proposed.[9] The advantage of the hexagonal model is that it allows for modeling of more packed cellular configuration in a limit closer to 1. However, this is a more complicated and calculation consuming approach, which needs to be further generalized into the case of electrically interacting cells. Cardiac cells do not have an ideal hexagonal cross section either. In addition, our model allows for making cellular configuration with volume fraction near 0.7, which is close to cellular volume fraction of myocardial tissue. Concluding, the proposed model of infinite cylinders with a circular cross section is a reasonable first approximation to estimate an effect of cellular electrical interaction on its bulk dielectrical properties with cellular volume fraction close to that of myocardial tissue.

CONCLUSIONS

(1) The difference between the model of electrically noninteracting cells and the model of electrically interacting cells is inversely dependent on frequency. At biological values of cellular volume fraction near 0.7

TABLE 1. Cellular model parameters.

Index	Media	Re (ϵ)	Conductivity σ (Ω/m)
0	Intracellular	75.0	0.54
1	Membrane	11.3	0.628E−3
2	Extracellular	75.0	1.43
Cellular radius=5 μm		Membrane thickness=100 Å	

(packed configuration) the difference is up to 10%–15% in resistance and in ϵ' for frequencies near 0.1 MHz.

(2) At less packed configuration with smaller cellular volume fraction, the bulk dielectrical properties of cellular compositions are structure dependent (structural anisotropy) at low frequencies (<10 MHz).

(3) Experimental data for myocardial tissue and theoretical data, for both interacting and noninteracting models, reasonably agree at frequencies 1–100 MHz.

ACKNOWLEDGMENTS

This work was supported by a grant from the Carolinas HealthCare System Foundation through the Carolinas Medical Center and Carolinas Heart Institute. The authors gratefully acknowledge technical assistance in experimental procedure of Dr. Wendy Chen, Michelle Thompson, Gerald Antonio, and Jackie Kassell.

APPENDIX: PARAMETERS OF THE MODEL

The parameters of cellular model are summarized in Table 1. The membrane permittivity was calculated based on published values of membrane capacitance $1\mu F/cm^2$.[17,28] The intracellular and extracellular permittivities were chosen to be closer to properties of saline and plasma solutions. Keeping in mind that the reported value of plasma resistivity at body temperature is about 64 Ω cm, and whole blood resistivity (at high hematocrit of 87 and frequency 0.2 MHz) is about 80 Ω cm,[1] we used a mean values of about 70 Ω cm as an extracellular resistance, which leads to conductivity of 1.43/Ω/m.

The intracellular conductivity was calculated based on values of intracellular ion concentrations,[2] ion mobility coefficients,[5] and the fact that ion diffusion coefficients are reduced intracellular.[14] This calculation gives a value of intracellular conductivity of 0.54/Ω/cm.

REFERENCES

[1] Ackmann, J. J., M. A. Seitz, C. A. Dawson, and L. L. Hause. Specific impedance of canine blood. *Ann. Biomed. Eng.* 24:58–66, 1996.
[2] Cole, K. S. Membranes, Ions, and Impulses. Berkeley: Berkeley University of California Press, 1968.
[3] Demir, S. S., J. W. Clark, C. R. Murphey, and W. R. Giles. A mathematical model of a rabbit sinoatrial node cell. *Am. J. Physiol.* 266:C832–C854, 1994.
[4] Fallert, M. A., M. S. Mirotznik, S. W. Downing, E. B. Savage, K. R. Foster, M. E. Josephson, and D. K. Bogen. Myocardial electrical impedance mapping of ischemic sheep hearts and healing aneurisms. *Circulation* 87:199–207, 1993.
[5] Fizicheskie Velichiny, edited by I. S. Grigorieva and E. Z. Meylichova. Moscow: Energoatomizdat, 1991.
[6] Foster, K. R., and H. P. Schwan. Dielectric properties of tissues. In: Handbook of Biological Effects of Electromagnetic Fields, 2nd ed., edited by C. Polk and E. Postow. NY: CRC Press, 1996, pp. 25–102.
[7] Gabriel, C., S. Gabriel, and E. Corthout. The dielectric properties of biological tissues: I. Literature survey. *Phys. Med. Biol.* 41:2231–2249, 1996.
[8] Gabriel, S., R. W. Lau, and C. Gabriel. The dielectric properties of biological tissues: II. Measurements in the frequency range 10 Hz to 20 GHz. *Phys. Med. Biol.* 41:2251–2269, 1996.
[9] Gielen, F. L. H., H. E. P. Cruts, B. A. Albers, K. L. Boon, W. Walunga-de Jonge, and H. B. K. Boom. Model of electrical conductivity of skeletal muscle based on tissue structure. *Med. Biol. Eng. Comput.* 24:34–40, 1986.
[10] Grant, E. H., R. J. Sheppard, and G. P. South. Dielectric Behavior of Biological Molecules in Solution. Oxford: Clarendon Press, 1978.
[11] Guide for the Care and Use of Laboratory Animals of the National Academy Press. Washington, DC, 1996.
[12] Hanai, T., K. Asami, and N. Koizumi. Dielectric theory of concentrated suspensions of shell-spheres in particular reference to the analysis of biological cell suspensions. *Bull. Inst. Chem. Res., Kyoto Univ.* 57:297–305, 1997.
[13] Ivanov, E. A. Diffraction of Electromagnetic Waves on Two Bodies, Minsk, Nayka and Technology, 1968.
[14] Kay, H. P., E. R. Cardoso, and E. Shwedyk. Correlation of permittivity and water content during cerebral edema. *IEEE Trans. Biomed. Eng.* 46:9:1121–1128, 1999.
[15] Kuchmerisk, M. J., and R. J. Podolsky. Ionic mobility in muscle cell. *Science* 166:1297–1298, 1969.
[16] Landau, L. D. and E. M. Lifshitz. Electrodynamics of Continuous Media. 2nd ed. Oxford: Pergamon, 1984.
[17] Lee, E. R., T. R. Wilsey, P. Tarczy-Hornoch, D. S. Kapp, P. Fessenden, A. Lohrbach, and S. D. Prionas. Body conformable 915 MHz microstrip array applicators for large surface area hyperthermia. *IEEE Trans. Biomed. Eng.* 39:5:470–483, 1992.
[18] Leon, L. J., and F. A. Roberge. Direction characteristics of action potential propagation in cardiac muscle, *Circ. Res.* 69:2:378–395, 1991.
[19] Maxwell, J. C. A Treatise on Electricity and Magnetism. New York: Dover, 1954.
[20] Medical Applications of Microwave Imaging, edited by L. E. Larsen and L. M. Jacobi. New York: IEEE, 1986.
[21] Non-Invasive Thermometry of the Human Body, edited by M. Miyakawa and J. Ch. Bolomey. Boca Raton, FL: CRC Press, 1996.
[22] Biological Effects of Electromagnetic Radiation, edited by J. M. Osepchuk. New York: IEEE, 1984.
[23] Semenov, S. Y., R. H. Svenson, A. E. Bulyshev, A. E. Souvorov, A. G. Nazarov, Y. E. Sizov, A. E. Pavlovsky, V. Y. Borisov, B. A. Voinov, G. I. Simonova, A. N. Starostin, V. G. Posukh, G. P. Tatsis, and V. Y. Baranov. Three-dimensional microwave tomography: Experimental prototype of the system and vector Born reconstruction method. *IEEE Trans. Biomed. Eng.* 46:8:937–946, 1999.
[24] Semenov, S. Y., A. E. Bulyshev, A. E. Souvorov, A. G.

Nazarov, Y. E. Sizov, R. H. Svenson, V. G. Posukh, A. V. Pavlovsky, P. N. Repin, and G. P. Tatsis. Three dimensional microwave tomography: Experimental imaging of phantoms and biological objects. *IEEE Trans. Microwave Theory Tech.* 48:6:1071–1074, 2000.

[25] Semenov, S. Y., R. H. Svenson, and G. P. Tatsis. Microwave spectroscopy of myocardial ischemia and infarction. 1. Experimental study. *Ann. Biomed. Eng.* 28:48–54, 2000.

[26] Semenov, S. Y., R. H. Svenson, A. E. Bulyshev, A. E. Souvorov, A. G. Nazarov, Y. E. Sizov, V. G. Posukh, A. Pavlovsky, and G. P. Tatsis. Microwave spectroscopy of myocardial ischemia and infarction. 2. Biophysical reconstruction. *Ann. Biomed. Eng.* 28:55–60, 2000.

[27] Stuchly, M. A., and S. S. Stuchly. Dielectrical properties of biological substances—tabulated, *J. Microwave Power* 15:19–26, 1980.

[28] Weidmann, S., Electrical constant of trabecular muscle from mammalian heart, *J. Physiol. (London)* 210:1041–1054, 1970.

[29] Yoon, R. S., A. Czaya, H. C. Kwan, and M. L. G. Joy. Changes in the complex permittivity during spreading depression in rat cortex. *IEEE Trans. Biomed. Eng.* 46:11:1330–1338, 1999.